Minerals Engineering 145 (2020) 106091

Contents lists available at ScienceDirect

Minerals Engineering

journal homepage: www.elsevier.com/locate/mineng

A comparative study on a newly designed ball mill and the conventional ball mill performance with respect to the particle size distribution and recirculating load at the discharge end

Harish Hanumanthappa (Research scholar)[a,*], Harsha Vardhan[a], Govinda Raj Mandela[a], Marutiram Kaza[b], Rameshwar Sah[b], Bharath Kumar Shanmugam[a]

[a] Department of Mining Engineering, National Institute of Technology Karnataka, Surathkal, Mangalore 575025, India
[b] R & D and SS, JSW Steel Limited, Vijayanagar Works, P.O. Vidyanagar, Ballari, Karnataka 583275, India

ARTICLE INFO

Keywords:
Particle size distribution
Recirculating load
Lifters
Ball mill

ABSTRACT

The discharge end design of a ball mill plays an important role in discharging the desired particle sizes (−150 + 10 μm) and the percentage of recirculating load from the discharge end of the ball mill. In continuous wet ball mills, the composition of feed (hard ore or soft ore) to the mill varies continuously, leading to uncontrolled grinding in the mill. In view of this, a new design of the discharge mechanism has been implemented to remove the ground particles of desired particle size fraction with minimum recirculating load (+150 μm).

The results from the discharge end with lifters (closed and open) show that the particle size fraction obtained from the discharge end has a maximum percentage of desired particle size fraction when the mill is operating at 60% critical speed. Discharge end without lifters has an uncontrolled particle size distribution in the discharge and the percentage of desired-size particles discharged was found to be very less. Also, the percentage of the recirculating load is minimum in the case of discharge end with lifter design compared with discharge end without a lifter. Hence, a new design of lifters in the discharge end leads to the discharge of the desired particle size fraction with minimum recirculating load.

1. Introduction

In wet grinding mills, the flow of the material inside the mill is due to the existence of a gradient between the feed position and the discharge trunnion. In overflow mills, at the discharge end of the mill, the ground product is removed by overflowing in the discharge trunnion and the size of particles discharged from the mill depends on the design of the discharge trunnion. However, the discharge of desired-size particles from the mill depends on the operating parameters of the mill.

Pulp lifters are used to transport slurry from the feed to the discharge end through grate holes in the mill. At the discharge end of the mill, based on the requirement, different types of lifter designs are used. Earlier, to lift the pulp, “pan pulp lifters” were used (Mokken et al., 1975), however, their design prevented their usage especially during increasing pulp flow. In order to overcome this, pulp lifters with an advanced design were used at the peripheral or discharge end of the mill and were found to operate effectively with an increase in the pulp flow and have improved power utilisation (Mokken et al., 1975).

The main drawback of lifters is that the slurry held up inside the mill is high as lifters are always in contact with the slurry; thus, the complete flowback of slurry to the mill cannot be avoided. This increasing backflow and formation of a pool of slurry ultimately affect the grinding efficiency of the mill (Morrell and Stephenson, 1996).

Mishra and Rajamani (1992, 1994a, 1994b) used 2DMILL code to predict the effect of liners/lifters on the motion of the balls and the power drawn. Hlungwani et al. (2003) studied the effect of mill speed and lifter shape on power draw by using the Discrete Element Method (DEM) simulator Millsoft (2D), which can predict whether square lifters draw lesser power than trapezoidal lifters when the mill operates at a normal operating speed of production mill.

Latchireddi and Morrell (2003) stated that the lower discharge rates in grate-pulp lifter assemblies are due to the inherent drawbacks in both radial and curved pulp lifter, allowing a proportion of the slurry to flow back into the mill before being discharged. In this system of design, a minor part of the slurry flows back to the mill while the major part is discharged through the grate-pulp system. Also, at higher mill speeds (typically > 80% of the critical speed) in addition to the flowback, a part of the slurry is carried over to the inside of the pulp lifter, which

* Corresponding author at: Department of Mining Engineering, National Institute of Technology Karnataka, Surathkal, Mangalore 575025, India.
E-mail address: hari.harish86@gmail.com (H. Hanumanthappa).

https://doi.org/10.1016/j.mineng.2019.106091
Received 15 February 2019; Received in revised form 11 October 2019; Accepted 12 October 2019

further reduces the discharge rate (Latchireddi and Morrell, 2003). Furthermore, it has been demonstrated that the discharge rate, performance and effectiveness of mills are controlled by pulp lifters (Weerasekara and Powell, 2014).

Djordjevic et al. (2004) adopted the DEM particle flow code (3D) to study the effect of lifter height and mill speed on power draw and found that as the mill speed increases, the mill with lower lifter height draws more power, but the mill with higher lifter height draws less power. It was also recorded that when grinding smaller particles, the power consumed was high for a mill with different lifter heights compared to the one with similar lifter heights. Makokha and Moys (2007) used cone lifters at the discharge end of the mill and observed, improvement in the mill product discharge as compared to the mill operated without cone-lifters.

Mill speed significantly affects the behavior of a particle inside the mill when it rotates at different operating speeds. At a rotating rate of 75–80% critical speed of the mill, particle behavior is highly consistent due to particle trajectory (Bian et al., 2017). The lifter design also plays a very important role in the inconsistent particle trajectory falling position. The particle movement towards the discharge end reduces when the height of the lifter is bigger. The number of lifters also influences the particle stream flow inside the mill. More lifters increase cataracting of particles inside the mill, leading to an increasingly dense flow stream of particles (Bian et al., 2017).

Gutiérrez et al. (2018) used DEM to simulate the material transport of different lifter profiles in the mill and found that the material discharge flow is higher in the case of a mill with inclined and radial lifters compared to the one with straight and radial pulp lifters.

In summary, different types of lifters were used to analyse the power draw, the forces acting on the lifter bar, the wear rate affecting the service life of lifters, the overall charge motion and the velocity of a single ball inside the mill (Nierop et al., 2001; Dong and Moys, 2002; Kalala et al., 2005, 2008; Powell et al., 2011; Toor et al., 2013; Mulenga and Moys, 2014; Cleary, 2009, 2015). Based on the literature, very limited work has been carried out on the effect of lifter design on the discharge of desired particle size (−150 μm/+10 μm) and recirculating load (+150 μm) to the ball mill. In the present study, the effect of mill speed on the production of a given size range (−150 μm/+10 μm) and recirculating load (+150) was investigated on three types of discharge end mechanisms of a ball mill.

2. Experimental set-up

The new laboratory ball mill with classifier set-up, shown in Fig. 1, was specially fabricated for conducting experiments in the laboratory. It has a length of 2 m, a diameter of 1.5 m and is fitted with a newly designed discharge end with six shell lifters, as shown in Fig. 2a and b and Fig. 3a and b. The feed end of the rotating drum has an opening of 0.3 m to feed the sample. An external feeding stand with feeder in the opening is provided at the feed end of the rotating drum. The rotating mill is filled with three steel balls of sizes 25 mm, 40 mm and 50 mm with 45%, 40% and 15% weight percentage, respectively. For collecting the ground product, the discharge end of the mill is connected to the classifier section, as shown in Fig. 1. The classification unit consists of multiple chambers to filter out different sets of size fractions. Although the present design depicts a three-chamber system, it can have more chambers for any selected size classification requirement. The chambers in the classification unit are variable in volume and created using movable pistons. The number of chambers can be increased or decreased by changing the piston assembly. The positional displacement of the pistons is variable. The positional displacement of the first piston is defined by the volume to be collected from the mill outlet to the first chamber. The subsequent displacement of the pistons is defined by the calculated material volumes of the selected size to be collected and separated. The first squeeze piston (closest to the discharge trunnion) was fitted with a defined coarser size sieve to facilitate recirculation of the oversized material for further comminution. The undersize material from the first chamber is squeezed and let into the second chamber. The second squeeze piston was fitted with a defined finer size sieve to facilitate the separation of the desired oversized material for the pellet feed making. The undersize material from the second chamber is squeezed and let into the third chamber. The collected product in the classifier section is removed using the outlets, as shown in Fig. 1. The opening and closing discharge end consist of a cap connected to one end of the rod whilst the other end of the rod is connected to a flange with a locking system, as shown in Fig. 1. The discharge end of the mill is closed by a cap connected to the rod and by applying force to the flange, which lead to a linear moment of the rod inside the classifier section; then, the rod along the cap is moved up to the discharge end to close the mouth of the discharge end. Whenever the closing cap closes in on the discharge end of the mill, a locking system outside classifier section is used to lock the moment of the rod. For providing continuous feed to the mill, a pump set-up is used to pump the slurry from the feed sump to the rotating mill. The rotating drum is driven by a motor with variable speed. The rated power of the motor was 3.7 kW and the rated speed 1450 rpm. A gearbox was used to decrease the speed of the motor. The reduction ratio of the gearbox was found to be 1:7; thus, the speed of the motor was reduced to 200 rpm. The motor speed was controlled using a potentiometer.

2.1. Design of outlet discharge trunnion with lifter arrangement

In the present work, in order to improve the grinding equipment's performance, a special type of discharge end overflow trunnion was

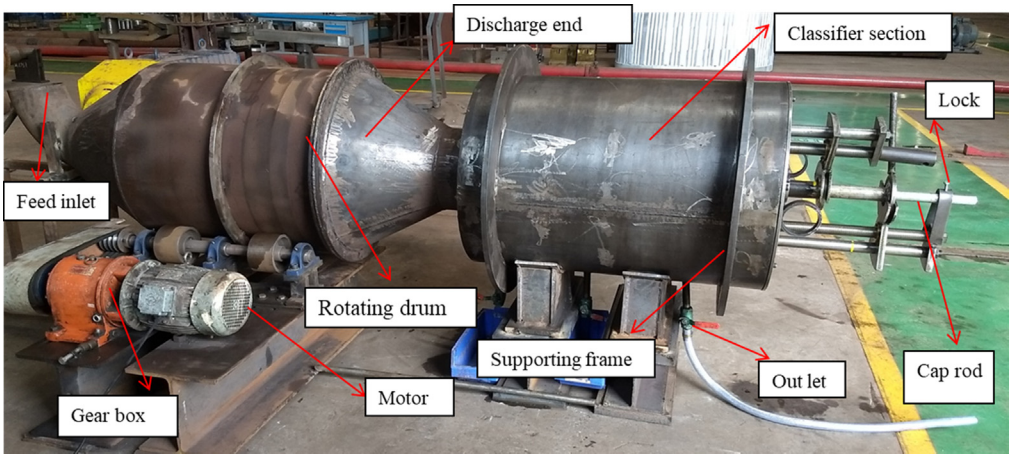

Fig. 1. Experimental setup of laboratory ball mill with classifier section.

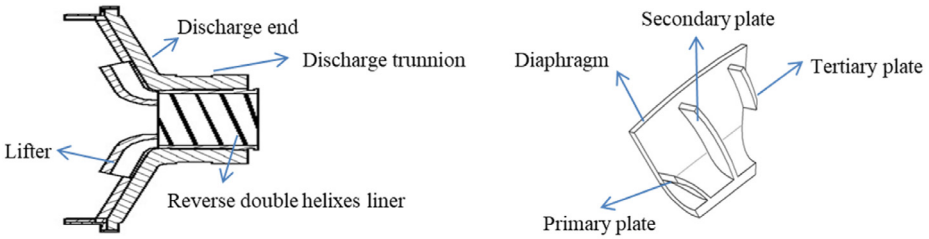

Fig. 2. (a) & (b). 2D view of the discharge end of the mill (after Nelson, 1980).

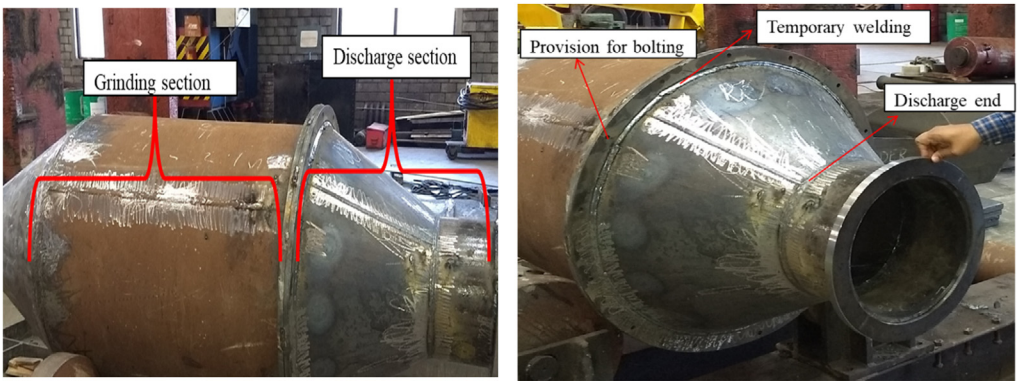

Fig. 3. (a) & (b). Ball mill with newly fabricated discharge end.

designed for fitting or removing lifters, as shown in Fig. 2a and b (Nelson, 1980). The ball mill was differentiated into two parts (Fig. 3a), the first part known as the grinding section and the second as the discharge section. Both parts are fabricated in such a way that they can easily be fitted by using bolts and nuts, as shown in Fig. 3b.

In this system, the slurry flows through the inlet feed trunnion due to the gradient between the inlet and outlet openings of the rotating drum. The inlet feed trunnion section is steeped with a higher angular position of 15–20° to the horizontal compared to discharge end overflow trunnion. The steeped angle at the inlet restricts backward flow and maintains better settling and enhanced initial acceleration to the material flow in the pulp. As shown in Fig. 2a, reverse double helixes in the discharge-end trunnion liner retains a major portion of the balls (grinding media) in the mill and discharges the pulp to the next section through the extended section of the discharge-end overflow trunnion.

Fig. 2b shows the lifter design with different orientation of lifter plates, which were installed at the discharge end of the experimental ball mill. A lifter plate mainly consists of primary, secondary and tertiary plates which are fixed and inclined at 30°, 35° and 30° respectively to the diaphragm plate. A total of six lifters were installed at the discharge end of the experimental ball mill. The lifter plates were made of rubber but they can also be made of other materials, such as PVC, steel, etc. The lifters were fitted at the discharge end of the ball mill using rivets. This shorter length of the lifter plates on the diaphragm acts as a separation zone from which fine particles are raised. Coarse particles and balls which enter the separation zone due to the tumbling action and gradient, and flow between the inlet and outlet of the mill are not carried by the lifter blades. This is because the lifter plates are inclined towards the mill section and of shorter length. The coarse particles and the balls are rolled back to the mill section.

2.2. Experimental procedure

Before starting the experiment, the chemical and physical composition of the selected iron ore sample was determined, as shown in Table 1. In the present study, the experiments were carried out at different discharge end operating conditions, as shown in Table 2. The discharge end was kept open for all the experiments in Case 1 and Case 2, as shown in Table 2. In Case 3, for all the experiments, the discharge end was kept open for 30 sec, during which the discharge particles were collected into the classifier unit. In Case 3, the discharge-end time was kept constant for all the experiments. After 30 sec, the mill discharge end was closed for another 30 sec by using a cap, during which the particles collected in the classification unit were removed and analysed. In Case 3, the discharge-end time was kept constant for all the experiments.

Table 1
Chemical and physical specification of iron ore sample.

Type of ore	Chemical Specification %				Grinding Specification	
Iron ore	Fe T	SiO_2	Al_2O_3	LOI	F_{80} (mm)	BWI(kWh/t)
	60.42	5.58	4.03	3.17	1.65	8.42

Initially, the mill discharge end is kept open by using an open-and-close mechanism at the discharge end. The mill is started by switching on the power button. The mill volume was maintained with 40% of charge throughout the experiment (Gupta and Yan, 2016). A rotating speed of 35.3 rpm, which corresponds to 100% of the mill's critical speed, was calculated using Eq. (1). The mill speed was varied from 20% to 70% of the critical speed of the mill with an interval of 10% mill critical speed, as shown in Table 2. Once the mill starts to rotate, it is fed with −3 mm particles size of iron ore slurry having a slurry density of 2.1 kg/m^3. For each critical speed, the mill was operated for 20 min. For the first 10 min of each critical speed, the mill was allowed to stabilise. During the stabilisation of the mill, the classifier section outlet valve of chamber one was kept open in order to remove the product discharged from the mill during the initial 10 min of grinding. After 10 min, the classification outlet valve was closed for another 10 min to collect the discharged product from the mill; once the mill reached a

Table 2
Experimental operating condition.

Constant Parameters	Varied Parameter	Different Operating Conditions		
		Case-1	Case-2	Case-3
Feed rate, Charge and Slurry density	Percentage of Critical speed (%) (20, 30, 40, 50, 60 & 70)	without lifters (cap open)	with lifters (cap open)	with lifters (cap closed)

stable condition. The collected samples were then removed from chamber one of the classifier section through the outlet valve and dried in the oven. After drying, a sample was collected for particle size analysis using a parallel beam laser diffraction set-up.

$$V_c = \frac{42.3}{\sqrt{D-d}} rev/min \quad (1)$$

where,

V_c = critical speed of the mill (in rpm);
D = the inner diameter of the mill (in meters); and
d = the size of the grinding balls (in meters).

2.3. Partial size measurements

The particle size measurement for the feed sample was conducted using a mechanical vibratory sieve shaker and the resultant PSD is presented in Fig. 4. The product particle size analysis was conducted using HELOS; a parallel beam laser diffraction set-up, which offers a powerful technology for particle size distribution analysis of powders, granules, suspensions, emulsions, sprays, and numerous other particulate systems. The particle size distribution ranging from 0.1 µm to 8750 µm can be considered for measurement. The equipment set-up is presented in Fig. 5.

The discharge product from the mill was dried in the oven. After drying, the samples were subjected to the parallel beam laser-diffraction set-up for particle size measurement. The particle size analysis obtained from the parallel beam laser-diffraction set-up is in terms of the cumulative passing particle size fraction. Based on the particle size analysis data, the size above +150 µm was considered as a recirculating load to the mill, the particle size range in −150 µm/+10 µm was considered as desired the size particles and particle size below −10 µm was considered as fine particles. This classification was done based on the different particle size range requirement for pellet feed. Pellet making requires feed particles to contain about 60–70% of 150–10 µm, less than 30% for particles smaller than 10 µm and no particles above 150 µm (Umadevi et al., 2013).

3. Results and discussions

The particle size distribution and percentage of the recirculating load obtained at the discharge were studied for different mill operating speeds, lifters and outlet-discharge mechanisms, as shown in Figs. 6–8.

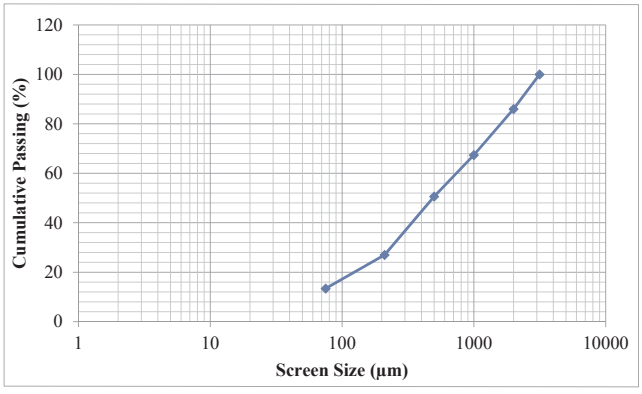

Fig. 4. Particle size analysis of feed sample.

Fig. 5. Particle size analyzer.

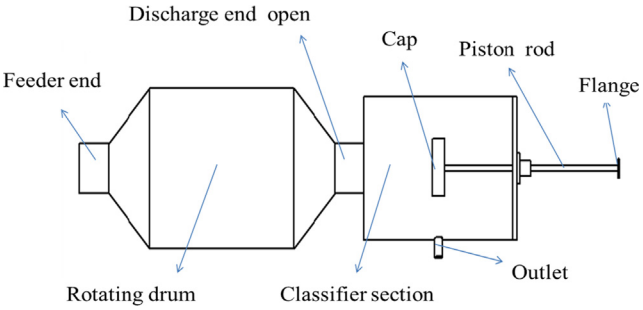

Fig. 6. Discharge end without lifters (discharge end open).

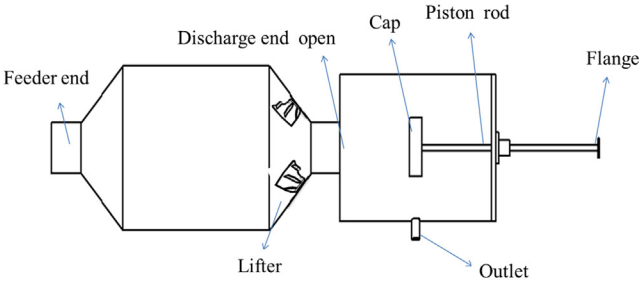

Fig. 7. Discharge end with lifters (discharge end open).

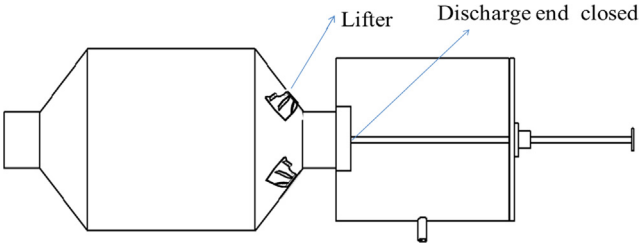

Fig. 8. Discharge end with lifters (discharge end closed).

The effect of the mill speed, with and without lifter arrangements at the discharge end of the mill, on the percentage of −150 µm particles passing, percentage of the recirculating load to the ball mill and passing particle size fraction at P_{80} is given in Table 3.

Table 3
Effect of mill speed, with and without lifter arrangements at the discharge end of the mill on percentage passing of −150 μm particle, percentage of recirculating load to the ball mill and passing particle size fraction at P_{80}.

Percentage of Critical speed (%)	% passing of −150 μm particle			% of recirculating load to the ball mill			Passing particle size fraction at P_{80} (μm)		
	Cap open		Cap closed	Cap open		Cap closed	Cap open		Cap closed
	without lifter	with lifter	with lifter	without lifter	with lifter	with lifter	without lifter	with lifter	with lifter
20	100	100	100	0	0	0	48	44	50
30	96	100	100	4	0	0	56	52	60
40	88	96	95	12	4	5	90	75	78
50	75	92	89	25	8	10	260	105	110
60	69	85	81	31	15	19	625	140	155
70	66	78	75	34	22	25	840	280	290

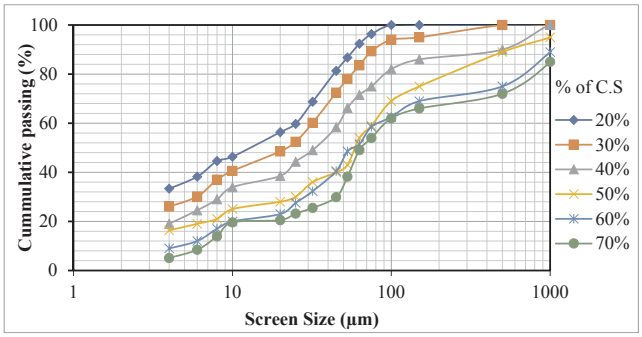

Fig. 9. Particle size analysis of discharge product when mill operated at different critical speeds (CS) without lifter and discharge end open.

3.1. Case 1: effect of mill speed on the product particle size distribution and recirculating load of the ball mill without lifters and the discharge end open

Particle size analysis was carried out by plotting the mesh size/screen size along the x-axis and the cumulative percentage passing along the y-axis. The results of particle size analysis are shown in Fig. 9, which shows particle size distribution obtained for each mill speed. A diagram relating to this portent is illustrated in Fig. 6. From Figs. 9 and 10, the particle size analysis results show that at a lower speed of the mill, very fine particles are discharged from the mill. This may be because at lower mill speed, particles with higher density in the slurry try to settle at the bottom of the shell and fine particles with lower density float on the upper surface of the slurry. Also, the particles move from bottom of the mill shell in anti-clock wise direction up to 3o'clock position, due to the cascading motion of particles and balls, where particles and balls cannot be further lifted up to shoulder position (Cleary, 2001c). Hence, the particles slip and slide back from the 3o'clock position to the grinding section because of gravity (Cleary, 2015). At lower mill speed, fine particles that are floating are discharged due to the gradient difference between the inlet and outlet of the mill. Thus, the ball mill works at relatively low efficiency at lower mill speed, since the majority of particles moving at a low speed in the grinding section will not collide with higher energy.

Fig. 10 shows the oversize (+150 μm), desired size (−150 μm/+10 μm) and undersize particle size (−10 μm) analysis of the discharge product when the mill is operating at different critical speeds without the lifter and the discharge end open. At 20% critical speed, about 81% of particle size distributions are fines, 19% is the desired size particles and no oversize particles were discharged. It is observed that, there was a variation of particle size distribution with each mill speed. At 60% of mill critical speed, the desired particle size distribution discharged from the mill was maximum compared to the mill operating at a different critical speed. However, above 60% of mill critical speed, there was an increase in the discharge percentage of oversize particles (+150 μm). This may be due to the fact that the mill without lifter arrangement in the discharge section cannot provide separation zone and leads to the discharge of maximum quantity of oversized particles. Also, the discharge end does not have any stopper to prevent unground particles from flowing back into the mill.

Fig. 11 shows the percentage of the recirculating load when the mill operates without the lifter and the discharge end is open. At the lower speed of the mill (less than 20% critical speed), the recirculating load is very low, since balls and the oversize particles in the mill will not rise up to shoulder position and will roll back to the bottom portion of the mill. This effect will reduce the grinding and also the recirculating load.

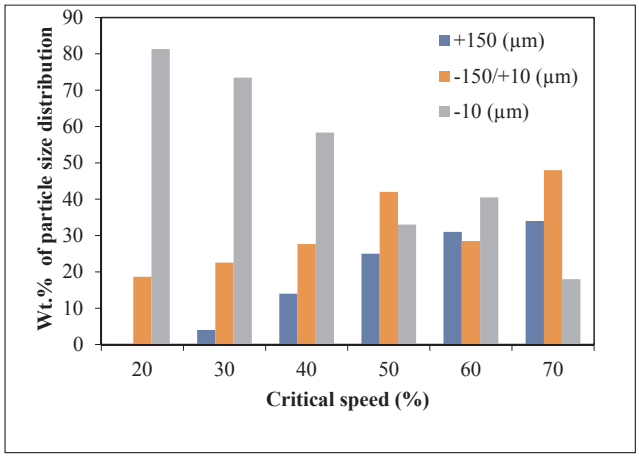

Fig. 10. Over size (+150 μm), narrow size (−150 μm/+10 μm) and undersize particle size (−10 μm) analysis of discharge product when mill operated at different critical speeds without lifter and discharge end open.

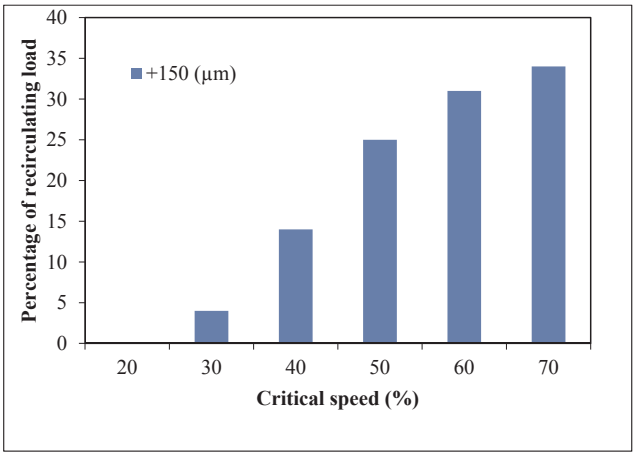

Fig. 11. Influence of mill speed on percentage of recirculating load when mill operated without lifter and discharge end open.

However, when the mill speed was increasing above 60% critical speed, it was observed that the recirculating load was also increasing. This was due to large quantities of unground particles moving at high speed and with less contact of particles with the mill shell that lift the particles and balls, and that in turn prevent the unground particles from flowing back into the grinding section, leading to the discharge of more unground particles from the mill (Gutiérrez et al., 2018). Hence, operating a ball mill without lifter is not preferable, since the grinding efficiency of the mill reduces and the particles discharged from the mill do not undergo size reduction. Also, the discharged particles consist of oversize particles, which are not suitable for pellet making; the load to the mill increases by recirculating the unground product to the mill.

3.2. Case 2: effect of mill speed on the particle size distribution of the product and the recirculating load of the ball mill with lifters and the cap open at the discharge

Lifter design and mill speed play a very important role in the flow and discharge of particles from the mill. Lifters are mainly used to lift particles from the toe end to the shoulder position of the shell. The falling trajectory of the particles from the shoulder position to the grinding section depends on the design of the lifters and the speed of the mill (Cleary, 2001c). Lifters can also transfer the motion from the mill shell into the motion of the particles (Djordjevic et al., 2004).

In this case, a special type of lifters was used in the discharge section of the mill. Each lifter consists of primary, secondary and tertiary plates. The primary plate was fixed at a corner portion of the diaphragm. The profile of the primary plate is concave, which acts as a bucket when the lifter reaches the bottom portion of the mill. This kind of profile helps lift the desired particles from the bottom portion of the mill to the discharge end of the mill. Having lifters at the discharge end avoids coarse particles and balls to exit from the discharge end. The lifter blades are arranged in such a way that whenever a stream of cataracting balls and coarse particles come in contact with the lifter blades, the blades direct the balls and coarse particles back to the grinding section instead of allowing them to enter the discharge trunnion. The lifter blades are designed in such a way that the outer radius of the blade is not extended but terminated inside (Fig. 2b). This design has a special zone known as the zone of separation at the conical portion of the discharge end of the mill, which helps lift desire-sized particles from the mill; however, balls and coarse-sized particles cannot be picked in the separation zone. A pictorial representation to ball mill with lifters and open cap at the discharge is shown in Fig. 7.

For all the experiments, the discharge end was kept open for varying speeds of the mill. The variation of the particle size distribution at the discharge for the mill operating at different speeds, with the discharge end fitted with lifters, is shown in Fig. 12. From Fig. 12, for a particular mill speed, there is a change in particle size distribution for the mill operating with lifters.

Fig. 13 shows the oversize (+150 μm), desire size (−150 μm/+10 μm) and undersize particle size (−10 μm) analysis of the discharge product when the mill is operating at different critical speeds with lifters and the discharge end open. According to Fig. 13, 70% instead of 60% critical speed seems to have produced the maximum amount of the desired size class. This may be due to the balls and particles' trajectory reaching at the discharge end began slipping from the shoulder position to the toe position when the mill was operated at 70% critical speed (Cleary, 2015; Bian et al., 2017). This kind of particle-profile stream at the discharge end helps the lifter plates classify the desired particle size range. The lifters are oriented in the grinding section in such a way that whenever the lifter reaches the bottom section of the mill shell, the primary plate lifts the selective-sized particles from the bottom end portion of the grinding chamber to the discharge end of the mill. Whereas, the secondary lifter plate, which is placed slightly away from the primary plate, lifts the particles present above the bottom section of the grinding end. The tertiary plate is placed at the inclined portion of the discharge end in such a way that it can help classify the particles. Hence, a new type of lifter design at the discharge end can be effectively used to classify the desire-sized particles from the mill.

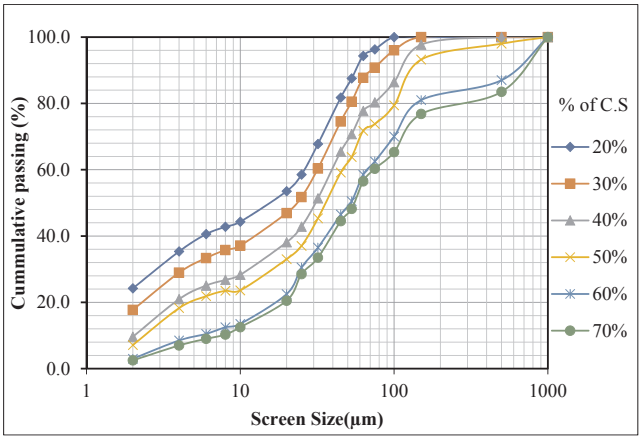

Fig. 12. Particle size analysis of discharge product when mill operated at different critical speeds (CS) with lifter and discharge end open.

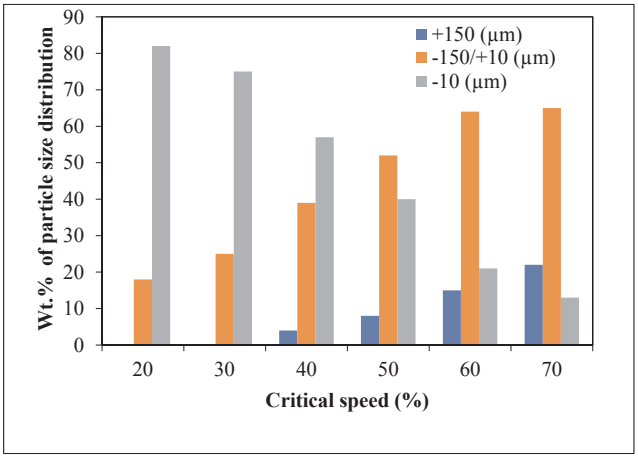

Fig. 13. Over size (+150 μm), narrow size (−150 μm/+10 μm) and undersize particle size (−10 μm) analysis of discharge product when mill operated at different critical speeds with lifter and discharge end open.

From Fig. 13, at lower mill speeds (20–30%), very fine particles were discharged from the mill, since a large proportion of the particles move at a relatively low speed and the discharge takes place due to the gradient difference between the inlet and outlet of the mill. At high mill speed (70%), the percentage of oversize particles discharged from the mill is high compared to 60% critical speed. This may be due to the particle trajectory reaching the discharge end with high speed at a higher shoulder position and eventually falls to the toe position when the mill was operated above 70% critical speed (Cleary, 2015; Bian et al., 2017). The high-speed particle profile at the discharge end may make it difficult for the lifters to classify desired particle size distribution since the velocity of the particles is high when the mill is rotating at high speed (Gutiérrez et al., 2018). Due to this, particles with high speeds have random motion at the discharge section, which leads to improper classification of particles in the lifters and leads to discharge of oversize particles from the discharge end without classification. Hence, at higher speeds of the mill, the percentage of oversize particles was higher than that of the desired particle size in the discharged product. The results suggest that, the new type of lifter design at discharge end can be effectively used to classify the desired size particles from the mill when the mill is operated at 70% of critical speed.

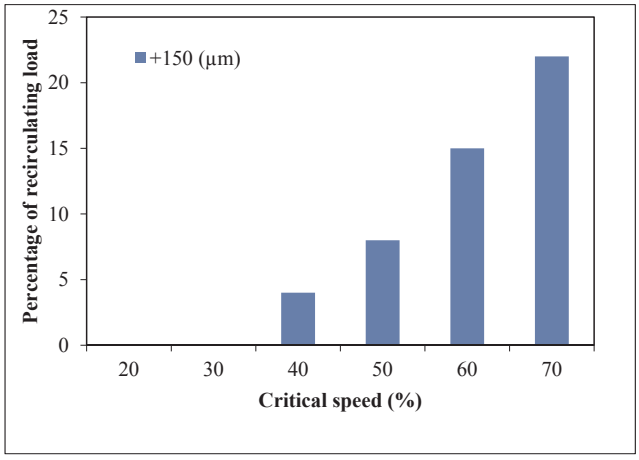

Fig. 14. Influence of mill speed on percentage of recirculating load when mill operated with lifter and discharge end open.

Fig. 14 shows the percentage of the recirculating load when the mill is operating with lifters and the discharge end is open. From Fig. 14, it is clear that with increasing mill speed, the recirculating load to the mill increases. The percentage of the recirculating load to the mill with lifters is less than the mill without lifters when the mill is operating at different critical speeds. There is about a 16% difference in the recirculating load between the mill with lifters and the one without.

3.3. Case 3: effect of mill speed on the particle size distribution and recirculating load in the ball mill with lifters and the cap closed at discharge

The opening and closing of the discharge end mechanism with lifters arrangement are shown in Fig. 8. In this case, the lifters used at the discharge end are the same as that of the previous case (Section 3.2, Case 2). In the previous two cases, the discharge end was kept open during the grinding operation. However, in this case, the discharge end was intermittently opened and closed for every 30 s while conducting the experiments. The opening and closing mechanism at the discharge end restricts slurry flow, leading to a lower rate of slurry discharge compared to the Case 1 and Case 2 mechanisms discussed earlier. Particle size distributions for different mill speeds are presented in Fig. 15.

Fig. 16 shows the oversize, the desired size range and undersize particle size analysis of the discharge product when the mill was operated at different critical speeds with lifters and the discharge end closed. Also, Fig. 17 shows the percentage of the recirculating load when the mill was operated with lifters and the discharge end open. The results of particle size distribution and recirculating load to the mill, as obtained in Case 3, are almost similar to that of Case 2, indicating that the closing and opening of the discharge end for every 30 s may not

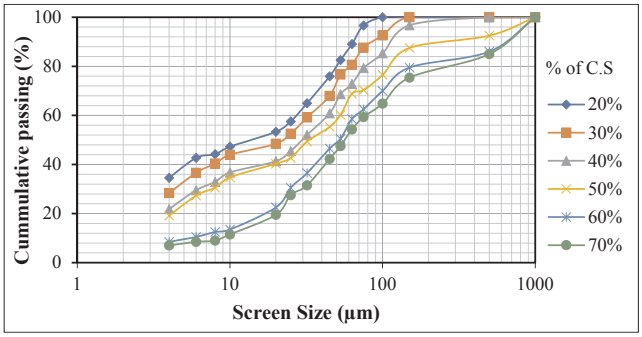

Fig. 15. Particle size analysis of discharge product when mill operated at different critical speeds (CS) with lifter and discharge end closed.

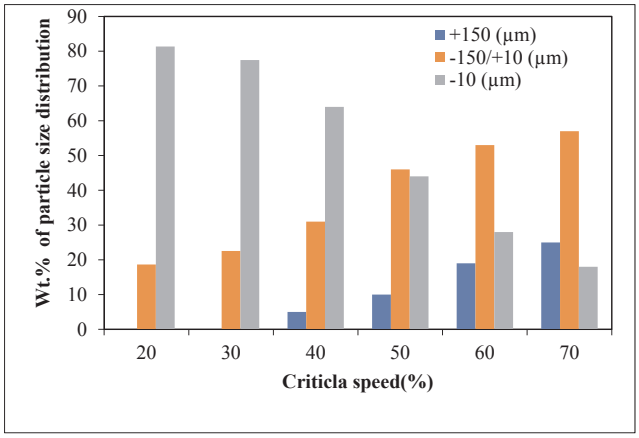

Fig. 16. Over size (+150 μm), narrow size (−150 μm/+10 μm) and undersize particle size (−10 μm) analysis of discharge product when mill operated at different critical speeds with lifter and discharge end closed.

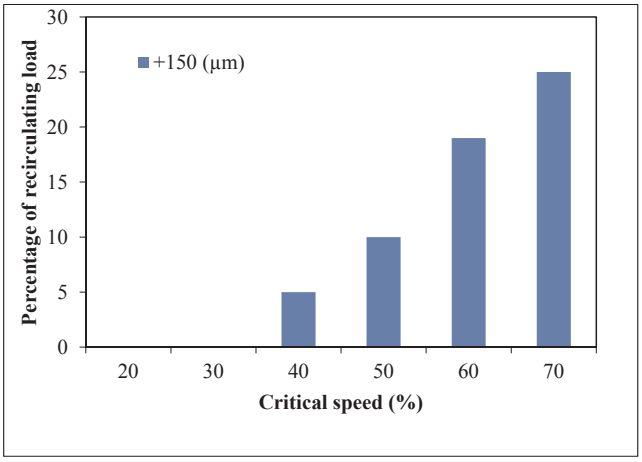

Fig. 17. Influence of mill speed on percentage of recirculating load when mill operated with lifter and discharge end closed.

have any effect on the particle size distribution from the discharge end of the mill.

3.4. Comparison of Case 1, Case 2 and Case 3

From Fig. 18(a & b), it is clear that the particle size distributions for Case 1, Case 2 and Case 3 are almost the same. The results obtained at 20% critical speed indicates that 80% passing size fraction in all the three cases is almost the same and that the particle size fraction at the discharge varies from 44 to 50 μm, as shown in Fig. 19. Also, from Fig. 20, at 20% critical speed, 100% passing size fraction in all the three cases is below 150 μm. This indicates that very low mill speeds do not have any impact on the size of the particles at the discharge end of the mill. The discharged products at lower mill speeds contain very fine particles, and the percentage of the desired particles discharged is very less (< 65%) than the required feed size range for pellet making.

The particle size distribution in Case 1 has more coarse particles in the range of 90–840 μm compared to Case 2 and Case 3, wherein the particle size ranges from 75 to 290 μm when the mill operates at 50–70% critical speed (Table 3, Fig. 18c–Fig. 15f, Fig. 19). The results of Case 2 and Case 3 indicate that the percentage of the desired particle size range discharged from the mill is well within the desired fraction (−150 μm/+10 μm); it is 65% when the mill is operating at 60% critical speed, as shown in Figs. 13 and 16. Also, in Case 1, when the mill is operating at 60% critical speed, the percentage of desired particle size

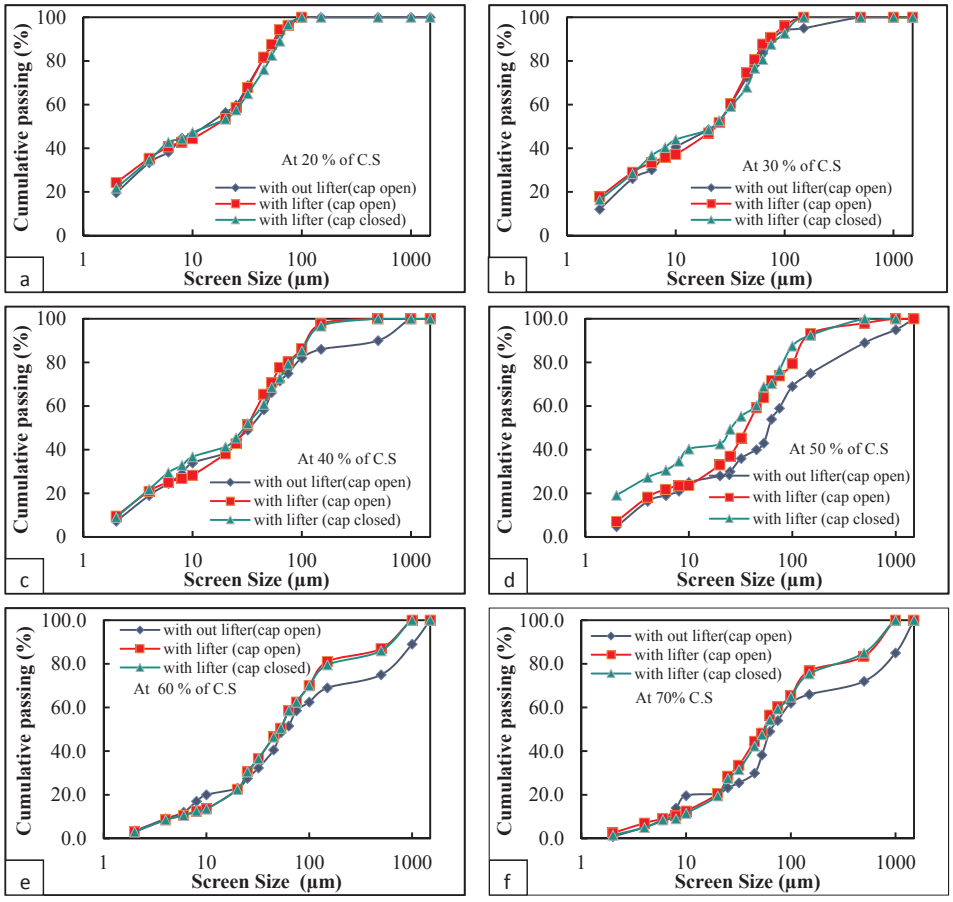

Fig. 18. Particle size distribution comparison for mill without lifter (cap open), with lifter (cap open), and with lifter (cap close) at different critical parentage speed (a) 20% of C.S, (b) 30% of C.S, (c) 40% of C.S, (d) 50% of C.S, (e) 60% of C.S, (f) 70% of C.S.

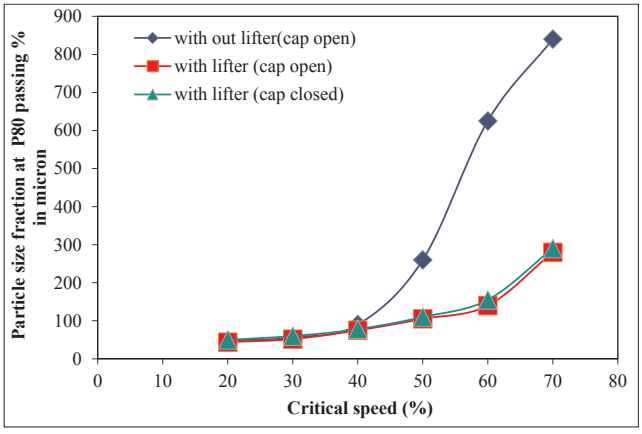

Fig. 19. Influence of mill speed on particle size fraction distribution with P_{80} passing percentage.

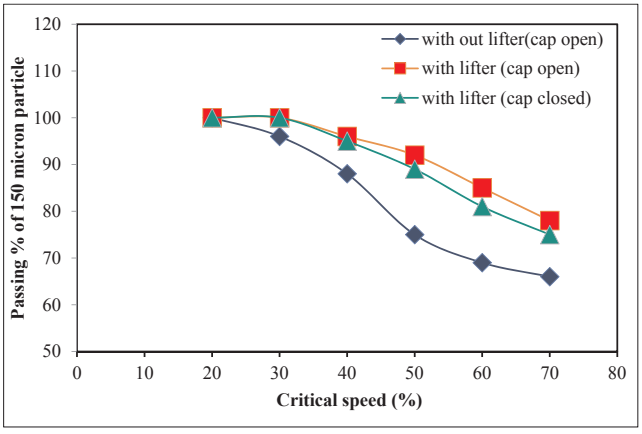

Fig. 20. Influence of mill speed on passing % of 150 µm particle.

range discharged from the mill is about 34% lesser than that of Case 2 and about 25% lesser than that of Case 3, as shown in Figs. 10, 13 and 16. The results indicate that the lifters at the discharged end play an important role in discharging the desired band particles when the mill is operated at a particular operating speed (60% critical speed). This is again due to lifters at the discharge end, which acts as a separation zone in the discharge end of the mill. However, mills without lifters at the discharge end lead to uncontrolled particle size distribution in the discharge product, since there is no barricade to stop the movement of unground particles at the discharge end of the mill. Hence, the discharge will consist of fines and unground particles, which are unsuitable for further processing.

It can be observed from Fig. 21 that for lower mill speeds of mills with and without lifters (open and closed condition) at the discharge end, a minimum percentage of the recirculating loads are yielded. A very smaller recirculating load was recorded at a mill speed of 20% with 80% passing particle size fraction varying from 44 to 50 µm, as shown in Table 3, for all the three cases. In all the three cases, at a mill critical speed above 70%, the percentage of the recirculating load to the mill increased with the increasing speed of the mill, as shown in Fig. 21. In Case 2 and Case 3, the percentage of the recirculating load at 60% critical speed is 15% and 19%, respectively, which is smaller compared to Case 1 with 31% recirculating load, as shown in Table 3. It can also

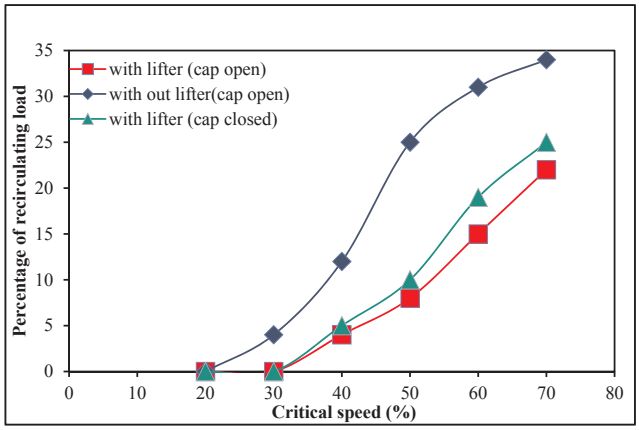

Fig. 21. Influence of mill speed on percentage of recirculating load to ball mill.

be observed that for all the three cases when the mill was operated above 60% critical speed, the recirculating load exceeded more than 20%, thus, an increase in the circulating load to the mill decreases the performance of the mill. The results suggest that well-designed lifters with proper orientation in the discharge end can help to discharge the desired particle size with minimum recirculating load.

4. Conclusions

A study of the laboratory ball mill performance for different mill speeds operating with and without lifters (cap open and cap close) at the discharge end has been presented in this paper. The behaviour of the ball mill with respect to the size of particles discharged and the percentage of the recirculating load to the mill was studied using this modified system. It was observed that a mill without a lifter arrangement in the diaphragm segment cannot provide a separation zone in the discharge end of the mill, which leads to uncontrolled particle size discharge from the mill; furthermore, the percentage of the desired particle sizes discharged was found to be very small. The mill with lifter arrangement in the diaphragm segment provided a separation zone in the discharge end of the mill that helped lift the desired particle sizes from the mill; however, balls and coarse size particles cannot be picked to the separation zone, leading to a relatively a higher percentage of the desired particle size distribution discharge from the mill. The following observations were made:

- The particle size distribution for Case 1, Case 2 and Case 3 was almost the same when the mill was operated at lower speeds (20–30% critical speed); 80% passing sizes of particles obtained at the discharge was composed of very fine particles of the range 44 to 50 μm.
- The discharge end without lifter arrangement led to a higher recirculating load of 34% when the mill was operated at 70% critical speed. At the same operating speed, the discharge end with lifter arrangements (Case 2 and Case 3) led to 22–25% recirculation, which is lesser compared with discharge end without a lifter.
- The discharge end with lifter arrangement discharged maximum percentage of the desired particle size with minimum percentage of recirculating load to the mill when the mill was operated at 60% critical speed.

The experimental results suggest that with appropriate design and placement of lifter in the discharge end, the output can attain the desired particle size distribution with the minimum recirculating load to the mill, ultimately decreasing the regrinding of ore in the mill.

Declaration of Competing Interest

The authors declared that there is no conflict of interest.

Acknowledgments

The authors sincerely thank the reviews who went paper in depth and provided valuable comments. The present research study was carried out in collaboration between NITK, Surathkal and JSW Steels, Ballari. The authors are thankful to the management of JSW Steels, Ballari for their support during the course of this research work. The authors would also like to thank the management of the Hutti Gold Mines Company Ltd. & Karnataka State Mineral Corporation Ltd. for their partial financial support for this work.

References

Bian, X., Wang, G., Wang, H., Wang, S., Lv, W., 2017. Effect of lifters and mill speed on particle behaviour, torque, and power consumption of a tumbling ball mill: experimental study and DEM simulation. Miner. Eng. 105, 22–35.
Cleary, P.W., 2001c. Charge behaviour and power consumption in ball mills: sensitivity to mill operating conditions, liner geometry and charge composition. Int. J. Miner. Process. 63, 79–114.
Cleary, P.W., 2009. Industrial particle flow modelling using discrete element method. Eng. Comput. 26, 698–743. https://doi.org/10.1108/02644400910975487.
Cleary, P.W., 2015. A multiscale method for including fine particle effects in DEM models of grinding mills. Miner. Eng. 84, 88–99. https://doi.org/10.1016/j.mineng.2015.10.008.
Djordjevic, N., Shi, F.N., Morrison, R., 2004. Determination of lifter design, speed and filling effects in AG mills by 3D DEM. Miner. Eng. 17, 1135–1142. https://doi.org/10.1016/j.mineng.2004.06.033.
Dong, H., Moys, M.H., 2002. Assessment of discrete element method for one ball bouncing in a grinding mill. Int. J. Miner. Process. 65, 213–226.
Gupta, A., Yan, D.S., 2016. Introduction to Mineral Processing Design and Operation, second ed. Elsevier.
Gutiérrez, A., Ahues, D., González, F., Merino, P., 2018. Simulation of material transport in a SAG mill with different geometric lifter and pulp lifter attributes using DEM. Mining, Metallurgy Exploration 36, 431–440.
Hlungwani, O., Rikhotso, J., Dong, H., Moys, M.H., 2003. Further validation of DEM modeling of milling: effects of liner profile and mill speed. Miner. Eng. 16, 993–998. https://doi.org/10.1016/j.mineng.2003.07.003.
Kalala, J.T., Breetzke, M., Moys, M.H., 2008. Study of the influence of liner wear on the load behaviour of an industrial dry tumbling mill using the Discrete Element Method (DEM). Int. J. Miner. Process. 86, 33–39. https://doi.org/10.1016/j.minpro.2007.10.001.
Kalala, J.T., Bwalya, M.M., Moys, M.H., 2005. Discrete element method (DEM) modelling of evolving mill liner profiles due to wear. Part I: DEM validation. Miner. Eng. 18, 1386–1391. https://doi.org/10.1016/j.mineng.2005.02.009.
Latchireddi, S., Morrell, S., 2003. Slurry flow in mills: grate-pulp lifter discharge systems (Part 2). Miner. Eng. 16, 635–642. https://doi.org/10.1016/S0892-6875(03)00135-3.
Makokha, A.B., Moys, M.H., 2007. Effect of cone-lifters on the discharge capacity of the mill product: Case study of a dry laboratory scale air-swept ball mill. Miner. Eng. 20, 124–131. https://doi.org/10.1016/j.mineng.2006.07.010.
Mishra, B.K., Rajamai, R.K., 1994b. Simulation of charge motion in ball mills. Part 2: numerical simulations. Int. J. Miner. Process. 40, 187–197.
Mishra, B.K., Rajamani, R.K., 1992. The discrete element method for the simulation of ball mills. Appl. Math. Model. 16, 598–604.
Mishra, B.K., Rajamani, R.K., 1994a. Simulation of charge motion in ball mills. Part 1: experimental verifications. Int. J. Miner. Process. 40, 171–186.
Mokken, A.H., Eng, B.S., Fellow, R., 1975. A study of the arrangements for pulp discharge on pebble mills, and their influence on mill performance. J. South African Inst. Min. Metall. 257.
Morrell, S., Stephenson, I., 1996. Slurry discharge capacity of autogenous and semi-autogenous mills and the effect of grate design. International Journal of Mineral Processing 46 (1–2), 53–72. https://doi.org/10.1016/0301-7516(95)00060-7.
Mulenga, F.K., Moys, M.H., 2014. Effects of slurry filling and mill speed on the net power draw of a tumbling ball mill. Miner. Eng. 56, 45–56. https://doi.org/10.1016/j.mineng.2013.10.028.
Nelson, J.E., 1980. Grinding mill diaphragm discharge system. United States Patent No. 4185786.
Nierop, M.A.Van, Glover, G., Hinde, A.L., Moys, M.H., 2001. A discrete element method investigation of the charge motion and power draw of an experimental. Int. J. Miner. Process. 61, 77–92.
Powell, M.S., Weerasekara, N.S., Cole, S., Laroche, R.D., Favier, J., 2011. DEM modelling of liner evolution and its influence on grinding rate in ball mills. Miner. Eng. 24, 341–351. https://doi.org/10.1016/j.mineng.2010.12.012.
Toor, P., Franke, J., Powell, M., Bird, M., Waters, T., 2013. Designing liners for performance not life. Miner. Eng. 43–44, 22–28. https://doi.org/10.1016/j.mineng.2012.07.004.
Umadevi, T., Kumar, M.G.S., Kumar, S., Prasad, C.S.G., Ranjan, M., 2013. Influence of raw material particle size on quality of pellets Influence of raw material particle size on quality of pellets. Ironmaking Steelmaking 35, 327–336. https://doi.org/10.1179/174328108X287928.
Weerasekara, N.S., Powell, M.S., 2014. Performance characterisation of AG / SAG mill pulp lifters using CFD techniques. Miner. Eng. 63, 118–124. https://doi.org/10.1016/j.mineng. 2014.02.001.